

Responses of hadrons to chemical potential at finite temperature

QCD-TARO Collaboration

S. Choe¹, Ph. de Forcrand^{2,3}, M. García Pérez³, S. Hioki⁴, Y. Liu¹, H. Matsufuru⁵,
O. Miyamura¹, A. Nakamura⁶, I. -O. Stamatescu^{7,8}, T. Takaishi⁹, T. Umeda¹⁰

¹*Dept. of Phys., Hiroshima Univ., Higashi-Hiroshima 739-8526, Japan*

²*Institut für Theoretische Physik, ETH-Hönggerberg, CH-8093 Zürich, Switzerland*

³*Theory Division, CERN, CH-1211 Geneva 23, Switzerland*

⁴*Dept. of Phys., Tezukayama Univ., Nara 631-8501, Japan*

⁵*Yukawa Institute for Theoretical Physics, Kyoto Univ. Kyoto 606-8502, Japan*

⁶*IMC, Hiroshima Univ., Higashi-Hiroshima 739-8521, Japan*

⁷*Institut für Theoretische Physik, Univ., Heidelberg, D-69120 Heidelberg, Germany*

⁸*FEST, Schmeilweg 5, D-69118 Heidelberg, Germany*

⁹*Hiroshima Univ. of Economics, Hiroshima 731-0192, Japan*

¹⁰*Center for Computational Phys., Univ. of Tsukuba, Tsukuba, Ibaraki 305-8577, Japan*
(February 5, 2020)

Abstract

A formulation to obtain the response of hadron masses to the chemical potential is developed on the lattice. As a first trial, screening masses of pseudoscalar and vector mesons and their responses are evaluated. We present results for two flavors of staggered fermions below and above T_c . The responses to both the isoscalar and isovector chemical potentials are sizable. They show different behaviours in the low and high temperature phases, which may be explained as a consequence of chiral symmetry breaking and restoration.

I. INTRODUCTION

It is well known that studying finite density QCD through lattice simulations is a very hard problem. The fermionic determinant at finite chemical potential is complex, and it gives an oscillating behaviour in quantum averages, making simulations very inefficient. The naive quenched approximation at finite chemical potential leads to an essentially different world [1], so that the use of dynamical fermions seems essential to extract the relevant physics. In spite of such a difficult situation, the study of the behaviour of hadrons in a finite baryonic environment is very important [2–4], especially in view of the evidences for deconfinement of quarks and gluons recently reported in high energy heavy ion collisions [5]. Moreover, some experimental results can be interpreted by assuming a shift in the mass and the width of the ρ meson, induced by the dense nuclear medium even below the deconfinement transition [6]. We are taking first steps towards studying such effects on the lattice here.

There are several approaches to circumvent the difficulty of studying a finite chemical potential system, and they seem successful to a limited extent [7,8]. In particular, the baryon number susceptibility at zero baryon density has been studied and an abrupt jump at the transition temperature has been reported [9]. There is in fact much interesting physical information which can be extracted from the behaviour of a system at small chemical potential. In this paper, we examine the behaviour of hadron masses in the vicinity of zero chemical potential at finite temperature. Our strategy is based on describing the response of hadrons to chemical potential by a Taylor expansion of hadronic quantities around $\mu = 0$. This allows simulations to be performed with standard methods at $\mu = 0$. Although a Taylor expansion cannot reproduce the non-analyticity inherent to a phase transition, it may suffice for observing the rounded, analytic behaviour indicative of a phase transition in a finite volume. Preliminary results of such a strategy can be found in [10,11].

The organization of this paper is as follows. In Sect.II, we develop basic formulae to evaluate the first and second responses of hadron masses with respect to both isoscalar and isovector chemical potentials. In Sect.III, we present and discuss some data obtained from Monte Carlo (MC) calculations. Conclusions are presented in Sect.IV.

II. CHEMICAL POTENTIAL RESPONSE OF HADRON MASSES AND RESIDUES AT HIGH TEMPERATURE

The basic framework is as follows. We aim at extracting the response of masses to chemical potential through an expansion of the form:

$$\left. \frac{M(\mu)}{T} \right|_{\mu} = \left. \frac{M}{T} \right|_{\mu=0} + \left(\frac{\mu}{T} \right) \left(\frac{dM}{d\mu} \right)_{\mu=0} + \left(\frac{\mu}{T} \right)^2 \frac{T}{2} \left(\frac{d^2 M}{d\mu^2} \right)_{\mu=0} + \mathcal{O} \left(\left(\frac{\mu}{T} \right)^3 \right) \quad (1)$$

at fixed temperature, T , and bare quark masses.

Suppose that a hadron correlator is dominated by a single pole¹

$$C(x) = \sum_{y,z,t} \langle H(x,y,z,t) H(0,0,0,0)^\dagger \rangle = \frac{\hat{\gamma}}{2\hat{M}} (e^{-\hat{M}\hat{x}} + e^{-\hat{M}(L_x - \hat{x})}) \quad , \quad (2)$$

where $\hat{M} = aM$ and $\hat{x} = x/a$. L_x is the lattice size in the x -direction. $\hat{\gamma}$ is the residue appearing in the propagator as $\gamma/(p^2 + m^2)$. In the following, we write $A = \hat{\gamma}/2\hat{M}$. The value of A depends on the choice of sources. But its behaviour as a function of the chemical potential provides information on the coupling to the medium.

We take the first and second derivatives with respect to $\hat{\mu} \equiv a_t \mu = \mu/(N_t T)$ where μ is the chemical potential;

$$C(x)^{-1} \frac{dC(x)}{d\hat{\mu}} = A^{-1} \frac{dA}{d\hat{\mu}} + \frac{d\hat{M}}{d\hat{\mu}} \left[\left(\hat{x} - \frac{L_x}{2} \right) \tanh \left(\hat{M} \left(\hat{x} - \frac{L_x}{2} \right) \right) - \frac{L_x}{2} \right] \quad (3)$$

¹Generalisation to a multi-pole situation is straightforward.

and

$$\begin{aligned}
C(x)^{-1} \frac{d^2 C(x)}{d\hat{\mu}^2} &= A^{-1} \frac{d^2 A}{d\hat{\mu}^2} \\
&+ (2A^{-1} \frac{dA}{d\hat{\mu}} \frac{d\hat{M}}{d\hat{\mu}} + \frac{d^2 \hat{M}}{d\hat{\mu}^2}) [(\hat{x} - \frac{L_x}{2}) \tanh(\hat{M}(\hat{x} - \frac{L_x}{2})) - \frac{L_x}{2}] \\
&+ (\frac{d\hat{M}}{d\hat{\mu}})^2 [(\hat{x} - \frac{L_x}{2})^2 + \frac{L_x^2}{4} - L_x(\hat{x} - \frac{L_x}{2}) \tanh(\hat{M}(\hat{x} - \frac{L_x}{2}))] \quad . \quad (4)
\end{aligned}$$

$C(x)$ and the first and the second derivatives of $C(x)$ are calculated from lattice simulations. Then, using the right-hand side of Eqs.(3) and (4), the first and the second responses of hadron masses and couplings are determined.

The next question is how to extract the derivative of the correlator from lattice simulations. For this purpose, we go back to the definition of the hadron correlator. In this work, we treat flavour non-singlet mesons in two flavour QCD. The hadron correlator is given by

$$\langle H(n)H(0)^\dagger \rangle = \langle G \rangle \quad , \quad (5)$$

where G is the meson propagator

$$G = \text{Tr}(g(\hat{\mu}_u)_{n0} \Gamma g(\hat{\mu}_d)_{0n} \Gamma^\dagger) \quad . \quad (6)$$

Here $g(\hat{\mu})$ is the quark propagator at finite chemical potential, and Γ is the Dirac matrix which selects the desired meson quantum numbers. The relation between the quark propagator and the Dirac operator $D(\hat{\mu})$ is

$$g(\hat{\mu}) = D(\hat{\mu})^{-1}. \quad (7)$$

An expectation value $\langle O \rangle$ stands for

$$\langle O \rangle = \frac{\int [dU] O \Delta e^{-S_G}}{\int [dU] \Delta e^{-S_G}} \quad , \quad (8)$$

where S_g is the gluonic action and Δ is the fermion determinant

$$\Delta = \det(D(\hat{\mu}_u)) \det(D(\hat{\mu}_d)) \quad . \quad (9)$$

Then, the first and the second derivatives are

$$\frac{d}{d\hat{\mu}} \langle H(n)H(0)^\dagger \rangle = \langle \dot{G} + G \frac{\dot{\Delta}}{\Delta} \rangle - \langle G \rangle \langle \frac{\dot{\Delta}}{\Delta} \rangle \quad (10)$$

and

$$\begin{aligned}
\frac{d^2}{d\hat{\mu}^2} \langle H(n)H(0)^\dagger \rangle &= \langle \ddot{G} + 2\dot{G} \frac{\dot{\Delta}}{\Delta} + G \frac{\ddot{\Delta}}{\Delta} \rangle - 2\langle \dot{G} + G \frac{\dot{\Delta}}{\Delta} \rangle \langle \frac{\dot{\Delta}}{\Delta} \rangle \\
&- \langle G \rangle [\langle \frac{\ddot{\Delta}}{\Delta} \rangle - 2(\langle \frac{\dot{\Delta}}{\Delta} \rangle)^2] \quad , \quad (11)
\end{aligned}$$

where the dotted \dot{O} and \ddot{O} stand for the first and the second derivatives with respect to $\hat{\mu}$ of the operator O .

At zero chemical potential, we have simpler expressions since

$$\left\langle \frac{\dot{\Delta}}{\Delta} \right\rangle = 0 \quad \text{at} \quad \hat{\mu} = 0 \quad . \quad (12)$$

Eq.(12) corresponds to the fact that the average baryon number density is zero at $\hat{\mu} = 0$. Actually, we see that $d \det(D)/d\hat{\mu} = \text{Tr}[\dot{D}D^{-1}]\det(D)$ is anti-hermitian at $\hat{\mu} = 0$:

$$\text{Tr}[\dot{D}D^{-1}] = \text{Tr}[\dot{D}\gamma_5\gamma_5D^{-1}] = \text{Tr}[(-\gamma_5\dot{D}^\dagger)(D^\dagger)^{-1}\gamma_5] = -\text{Tr}[\dot{D}D^{-1}]^* \quad . \quad (13)$$

This means that $d \det(D)/d\hat{\mu}$ changes sign under the transformation $U \rightarrow U^\dagger$. Since the measure and the gluonic action are invariant under this transformation, its expectation value vanishes [12]. Thus, at zero chemical potential, Eqs.(10) and (11) turn into

$$\begin{aligned} \frac{d}{d\hat{\mu}} \langle H(n)H(0)^\dagger \rangle &= \langle \dot{G} + G \frac{\dot{\Delta}}{\Delta} \rangle \quad , \\ \frac{d^2}{d\hat{\mu}^2} \langle H(n)H(0)^\dagger \rangle &= \langle \ddot{G} + 2\dot{G} \frac{\dot{\Delta}}{\Delta} + G \frac{\ddot{\Delta}}{\Delta} \rangle - \langle G \rangle \left\langle \frac{\ddot{\Delta}}{\Delta} \right\rangle \quad . \end{aligned} \quad (14)$$

We investigate derivatives with respect to both isoscalar and isovector type of chemical potentials. The isoscalar chemical potential is conjugate to the total quark density. In this paper we study the response to the isoscalar chemical potential by setting

$$\hat{\mu}_S = \hat{\mu}_u = \hat{\mu}_d \quad , \quad (15)$$

and for the isovector case

$$\hat{\mu}_V = \hat{\mu}_u = -\hat{\mu}_d \quad . \quad (16)$$

Note that Son and Stephanov proposed a model corresponding to the isovector case as a good test bed for chemical potential effects in QCD [13]. The advantage of setting $\hat{\mu}_u = -\hat{\mu}_d$ is that the fermion determinant is positive, so that the problem becomes tractable with standard lattice techniques. Here we don't make use of this advantage and still study the dependence on $\hat{\mu}_V$ by performing a Taylor expansion around $\hat{\mu}_V = 0$. Future simulations at non-zero $\hat{\mu}_V$ will also constitute a good test of the performance of our Taylor expansion approach.

Our simulations with $n_f = 2$ dynamical quarks are performed using staggered fermions. The fermion operator and its derivatives are

$$\begin{aligned} D(U, \hat{\mu})_{n,m} &= m a \delta_{n,m} + \frac{1}{2} \sum_{\sigma=x,y,z} \eta_\sigma(n) [U_{\hat{\sigma}}(n) \delta_{n+\hat{\sigma},m} - U_{\hat{\sigma}}^\dagger(n - \hat{\sigma}) \delta_{n-\hat{\sigma},m}] \\ &\quad + \frac{1}{2} \eta_t(n) [U_{\hat{t}}(n) e^{\hat{\mu}} \delta_{n+\hat{t},m} - U_{\hat{t}}^\dagger(n - \hat{t}) e^{-\hat{\mu}} \delta_{n-\hat{t},m}] \quad , \end{aligned} \quad (17)$$

$$\frac{dD}{d\hat{\mu}} = \frac{1}{2} \eta_t(n) [U_{\hat{t}}(n) e^{\hat{\mu}} \delta_{n+\hat{t},m} + U_{\hat{t}}^\dagger(n - \hat{t}) e^{-\hat{\mu}} \delta_{n-\hat{t},m}] \quad , \quad (18)$$

and

$$\frac{d^2 D}{d\hat{\mu}^2} = \frac{1}{2} \eta_t(n) [U_{\hat{t}}(n) e^{\hat{\mu}} \delta_{n+\hat{t},m} - U_{\hat{t}}^\dagger(n - \hat{t}) e^{-\hat{\mu}} \delta_{n-\hat{t},m}] \quad , \quad (19)$$

where $\hat{\sigma}$ and \hat{t} are unit vectors pointing along space and time directions.

Taking into account the four-fold degeneracy of the staggered fermion operator, the determinant factor Δ of $n_f = 2$ fermions is then

$$\Delta = \exp\left[\frac{1}{4} \text{Tr} \ln D(U, \hat{\mu}_u) + \frac{1}{4} \text{Tr} \ln D(U, \hat{\mu}_d)\right] \quad . \quad (20)$$

Explicit formulae are given in Appendix A (for the isoscalar case) and B (for isovector), and specialized for staggered fermions in Appendix C.

III. NUMERICAL RESULTS

In this study, simulations are performed on a $16 \times 8^2 \times 4$ lattice. We study responses of hadrons below and above the confinement/deconfinement phase transition temperature. For two light flavours of staggered fermions, the critical coupling β_c at $N_t = 4$ is $\beta_c = 5.271$ for $ma = 0.0125$, and $\beta_c = 5.288$ for $ma = 0.025$ [14,15]. Our simulations are carried out with the R-algorithm. The time step of the molecular dynamics is taken as $\delta = 0.01$, and the trajectory length is 50 steps. We measure correlators on configurations separated by 20 trajectories. To evaluate the traces of the various fermionic operators, the Z_2 noise method [16] is used, with 200 noise vectors. Hadronic correlators are measured by using the corner-type wall source [17] after Coulomb gauge fixing in each x -hyperplane, and we choose three quark masses, $ma = 0.0125, 0.017, 0.025$. The parameters of our simulations, including the number of configurations used in each case for our analysis, are summarized in Table I. The average Polyakov loop is shown in Fig.1. It shows that, for each quark mass, we cover temperatures on either side of the phase transition.

Many terms contribute to the derivatives of the meson correlator with respect to the chemical potential: see Eqs.(B5), (C2), and (C3) in the Appendix. Representative terms are:

$$\begin{aligned} (A) : & 2 \sum_{y,z,t} \text{Re} \langle \text{Tr} |(g \dot{D} g)_{n0}|^2 \rangle \\ (B) : & 4 \sum_{y,z,t} \text{Re} \langle \text{Tr} [(g \dot{D} g \dot{D} g)_{n0} g_{n0}^\dagger] \rangle \\ (C) : & 2 \sum_{y,z,t} \text{Re} \langle \text{Tr} [(g \ddot{D} g)_{n0} g_{n0}^\dagger] \rangle \quad . \end{aligned} \quad (21)$$

In Fig.2, we show the pseudoscalar correlator. Error bars are clearly very small. Nevertheless, a single pole fit works very well over the interval $1 < x/a < 15$. We also present in the figure the terms (A), (B) and (C) above. All of them can be determined with reasonable accuracy.

Let us turn to the first response of the pseudoscalar correlator to the chemical potential. Note that the first derivative with respect to the isoscalar chemical potential is identically zero (see Eq.(A9) in Appendix A). For the isovector chemical potential, Fig.3 shows

$C^{-1}dC/d\hat{\mu}_V$ at $\beta = 5.26$ and 5.34 . At both temperatures, the values are very small. This is consistent with a comparative study in the Nambu–Jona-Lasinio (NJL) model, which also predicts very small responses around the critical temperature [19].

We consider then the second responses, starting with the pseudoscalar meson channel. Fig.4 shows $C^{-1}d^2C/d\hat{\mu}^2$ at $\beta = 5.26$ (below β_c) and 5.34 (above β_c) for the isoscalar and isovector chemical potentials. The solid curves are fits by Eq.(4), after fitting $C(x)$ by Eq.(2).

We determine the dependence of a meson mass on the chemical potential as follows. (i) First we determine the meson mass \hat{M} by the usual step. Namely, we fit the MC results of the correlator to Eq.(2). The value of the meson mass \hat{M} is obtained as a fitting parameter. (ii) Then we fit the MC results for the derivatives of the meson correlator to Eqs.(3) and (4), substituting in them the value previously determined for \hat{M} . The derivatives of masses and coupling are then obtained as fitting parameters. Note that for $\hat{\mu}_S$ we omit the fitting step to Eq.(3) since the first response is strictly zero.

A. Responses of the pseudoscalar meson mass to the isoscalar chemical potential

Results of the pseudoscalar meson response to the isoscalar chemical potential are summarized in Table II. The screening mass of the pseudoscalar meson at $ma = 0.025$ as a function of T/T_c is shown in Fig.5 .

In the low temperature phase, the dependence of the mass on $\hat{\mu}_S$ is small. This behaviour is to be expected since, below the critical temperature and in the vicinity of zero $\hat{\mu}_S$, the pseudoscalar is still a goldstone boson. In fact, if the chiral extrapolation is made, the limiting value of the isoscalar response is consistent with zero as shown in Fig.6. This is in contrast with the picture above T_c where, even in the chiral limit, $d^2\hat{M}^2/d\hat{\mu}^2$ remains large. In addition, our results suggest that the response of the coupling is small below T_c .

Above T_c , we first note that the correlator and its response are still well fitted by single pole formulae, Eqs.(2-4). Screening masses are manifestly larger than those below T_c . This confirms results of previous works [9]. As pointed before, the response of the mass above T_c becomes large, a reflection of the fact that the pion is no longer a goldstone and an indication of chiral symmetry restoration. We also note that the response of the coupling increases, which could reflect a larger projection onto free quarks as described by the wall-source.

B. Responses of the pseudoscalar meson mass to the isovector chemical potential

Results for the isovector chemical potential are summarized in Table III. In the presence of the isovector chemical potential, π^+ and π^- may have different masses. Here we consider the π^+ ($u\bar{d}$) meson as shown in Eq.(6). In contrast to the case of the isoscalar chemical potential, the second order response of the mass is significantly large in the low temperature phase, and decreases in magnitude above T_c . The difference between the isoscalar and isovector chemical potentials is illustrated in Fig.7. The response of the residue, $\hat{\gamma}$, also

shows different behaviours in the confined and deconfined phases, illustrated in Fig.8. ²

These features are manifest even for a small quark mass parameter. Note that the isovector potential explicitly breaks the $u - d$ symmetry, even if the two quarks have equal masses. The phase structure in the $(T, |\mu_V|)$ plane has been studied by Son and Stephanov [13]. The original $SU(2)_{L+R}$ symmetry at non-zero quark mass and zero chemical potential is broken down to $U(1)_{L+R}$. At zero T and for $|\mu_V|$ larger than the mass of the pseudoscalar, the system is in a different phase from $\mu = 0$. The ground state is a pion condensate and there is one massless goldstone associated with the spontaneous breaking of the $U(1)_{L+R}$ symmetry. For $|\mu_V| = m_{PS}$, the critical temperature is $T = 0$. At sufficiently high temperature, the condensate melts and the symmetry is restored. Due to the presence of the phase boundary, we do not expect to be able to reach the condensed phase by Taylor expanding around $\mu_V = 0$. We can however hope to get some hints about the presence of the phase boundary while keeping $|\mu_V| < m_{PS}$. In this case, the system is in the same ground state as for zero chemical potential, there are no exact goldstone modes and the three pions are massive.

An interesting point in this respect is that the second derivative of the mass is negative in the low temperature phase, in marked contrast with what happened for the isoscalar potential. The mass tends to decrease under the influence of the isovector chemical potential, reflecting the fact that for low temperature and chemical potential above the pion mass, a goldstone appears [1,13]. This is more clearly shown by an expansion as in Eq.(1). At $\beta = 5.26$ and $ma = 0.017$, the data suggest

$$\frac{M(\mu_V)}{T}|_{\mu_V} = \frac{M}{T}|_{\mu_V=0} + (0.021 \pm 0.034)(\frac{\mu_V}{T}) - (1.31 \pm 0.04)(\frac{\mu_V}{T})^2 + O((\frac{\mu_V}{T})^3) \quad . \quad (22)$$

The coefficient of the linear term is consistent with zero. Notice also in Table III that the lighter the quark mass, the stronger the response, a possible indication that for lighter pions the phase boundary is closer to the zero chemical potential axis, as suggested in [13].

In the high temperature phase, the dependence of the masses on μ_V decreases. Since the pseudoscalar meson becomes heavier, the phase boundary to the pion condensate phase is farther away from the $\mu_V = 0$ axis. The weaker responses may be understood from this point of view.

C. Results for the vector meson

Vector meson correlators can be computed, but the signal to noise ratio for their response is very bad. An example is provided in Fig.9, for $\beta = 5.26$. At present, the screening mass and the responses are extracted from a limited range in x near the source, where the statistical error is smaller. The first order response to the isovector chemical potential is again small and consistent with zero. The second order response to the isoscalar chemical potential appears to be positive at low temperature, whereas that to the isovector potential is negative. In comparison with the pseudoscalar meson case, for example $d^2\hat{M}/d\hat{\mu}_V^2$, the responses are weak.

²Note that $(d^2\hat{\gamma}/d\hat{\mu}^2)/\hat{\gamma}$ does not depend on the choice of the source normalization.

Finally, let us turn to the high temperature phase. At $\beta = 5.34$, the correlator and its response show markedly different x -dependence, compared to the pseudoscalar meson. Apparently, formulae based on a single meson pole dominance, Eqs.(2-4), give very poor descriptions of the data. High statistics simulations shall be required to clarify the behaviour.

IV. CONCLUSIONS

In this work, we have developed a framework to study the response of hadrons to the chemical potential. It is based on Taylor expanding hadronic quantities around $\mu = 0$. We show the first results of the first and second derivatives of pseudoscalar and vector meson masses with respect to μ . As shown in the previous sections, the second order responses are sizable and reveal several characteristic features. For the pseudoscalar meson, the behaviour of the responses seems to have close contact to chiral symmetry restoration. For the isoscalar chemical potential μ_S , the dependence of the pseudoscalar mass on μ_S in the chiral limit is consistent with zero, reflecting the fact that at low temperature and small μ_S the pion is still a goldstone. For the isovector chemical potential, we show features that point towards the phase structure studied by Son and Stephanov [13]. The $u\bar{d}$ pseudoscalar mass tends to decrease as a function of μ_V at a much stronger rate in the low temperature phase.

It is notable that a single hadron pole gives a good description for the response as well as for the correlator at $\beta = 5.34$ ($T/T_c \approx 1.1$) in the pseudoscalar channel.

On the other hand, the results for the vector meson response are still too noisy. It is encouraging that the questions touched in the introduction appear to be addressable within our approach, but improved statistics are necessary for quantitative conclusions.

Since the present study is a first trial, our simulations have been performed on a rather small lattice. However, differences between the dynamics of $N_t = 4$ and $N_t = 6$ lattices have been reported [18]. Thus, further investigations on larger lattices are indispensable.

The chemical potential response of the nucleon is also an interesting issue. That of the quark condensate is even more important. An exploratory study on these topics is in progress.

ACKNOWLEDGMENTS

This work is supported by Grant-in-Aide for Scientific Research by Monbusho, Japan (No.11694085, No.11740159, and No. 12554008). Simulations were performed on the HI-TACHI SR8000 at IMC, Hiroshima University. H.M. is supported by the Japan Society for the Promotion of Science for Young Scientists.

APPENDIX A: FORMULAE FOR THE ISOSCALAR CHEMICAL POTENTIAL RESPONSE

Using Eq.(15), the quark propagator g satisfies the relation

$$g(\hat{\mu}_d)_{0n} = \gamma_5 g^\dagger(-\hat{\mu}_d)_{n0} \gamma_5 \quad , \quad (\text{A1})$$

so that the meson correlator G is given by

$$G = \text{Tr}[g(\hat{\mu}_S)_{n0}\Gamma\gamma_5 g(-\hat{\mu}_S)_{n0}^\dagger\gamma_5\Gamma^\dagger] \quad , \quad (\text{A2})$$

where Tr means the trace over spinor and colour indices. Each propagator is expanded as

$$\begin{aligned} g(\hat{\mu}) &= g - \hat{\mu}g\dot{D}g + \frac{\hat{\mu}^2}{2}(2g\dot{D}g\dot{D}g - g\ddot{D}g) + O(\hat{\mu}^3) \quad , \\ g(-\hat{\mu}) &= g + \hat{\mu}g\dot{D}g + \frac{\hat{\mu}^2}{2}(2g\dot{D}g\dot{D}g - g\ddot{D}g) + O(\hat{\mu}^3) \quad , \end{aligned} \quad (\text{A3})$$

where g and D are the propagator and the Dirac operator at zero chemical potential, respectively, and the relation

$$\dot{g} = -g\dot{D}g \quad (\text{A4})$$

is used.

The first derivative at $\hat{\mu}_S = 0$ is

$$\dot{G} = -i2\text{ImTr}[(g\dot{D}g)_{n0}\Gamma\gamma_5 g_{n0}^\dagger\gamma_5\Gamma^\dagger] \quad , \quad (\text{A5})$$

and the second derivative at $\hat{\mu}_S = 0$ is obtained as

$$\begin{aligned} \ddot{G} &= 4\text{ReTr}[(g\dot{D}g\dot{D}g)_{n0}\Gamma\gamma_5 g_{n0}^\dagger\gamma_5\Gamma^\dagger] - 2\text{ReTr}[(g\ddot{D}g)_{n0}\Gamma\gamma_5 g_{n0}^\dagger\gamma_5\Gamma^\dagger] \\ &\quad - 2\text{Tr}[(g\dot{D}g)_{n0}\Gamma\gamma_5 (g\dot{D}g)_{n0}^\dagger\gamma_5\Gamma^\dagger] \quad . \end{aligned} \quad (\text{A6})$$

Let us calculate the derivatives of Δ . Using the following equations ,

$$\begin{aligned} \frac{d}{d\hat{\mu}}\det(D) &= \text{Tr}[\dot{D}g]\det D \quad , \\ \frac{d^2}{d\hat{\mu}^2}\det(D) &= \{\text{Tr}[\ddot{D}g] - \text{Tr}[\dot{D}g\dot{D}g] + \text{Tr}[\dot{D}g]^2\}\det(D) \quad , \end{aligned} \quad (\text{A7})$$

we have

$$\begin{aligned} \frac{\dot{\Delta}}{\Delta} &= 2\text{Tr}[\dot{D}g] \quad , \\ \frac{\ddot{\Delta}}{\Delta} &= 2\text{Tr}[\ddot{D}g] - 2\text{Tr}[\dot{D}g\dot{D}g] + 4\text{Tr}[\dot{D}g]^2 \quad . \end{aligned} \quad (\text{A8})$$

Combining Eqs.(14), (A5), (A6), (A7) and (A8), we have

$$\frac{d}{d\hat{\mu}}\text{Re}\langle H(n)H(0)^\dagger \rangle = 0 \quad , \quad (\text{A9})$$

and

$$\begin{aligned} \frac{d^2}{d\hat{\mu}^2}\text{Re}\langle H(n)H(0)^\dagger \rangle &= 4\text{Re}\langle \text{Tr}[(g\dot{D}g\dot{D}g)_{n0}\Gamma\gamma_5 g_{n0}^\dagger\gamma_5\Gamma^\dagger] \rangle \\ &\quad - 2\text{Re}\langle \text{Tr}[(g\ddot{D}g)_{n0}\Gamma\gamma_5 g_{n0}^\dagger\gamma_5\Gamma^\dagger] \rangle \\ &\quad - 2\text{Re}\langle \text{Tr}[(g\dot{D}g)_{n0}\Gamma\gamma_5 (g\dot{D}g)_{n0}^\dagger\gamma_5\Gamma^\dagger] \rangle \\ &\quad + 8\langle \text{ImTr}[(g\dot{D}g)_{n0}\Gamma\gamma_5 g_{n0}^\dagger\gamma_5\Gamma^\dagger] \text{ImTr}[\dot{D}g] \rangle \\ &\quad + 2\text{Re}\{ \langle \text{Tr}[g_{n0}\Gamma\gamma_5 g_{n0}^\dagger\gamma_5\Gamma^\dagger] (\text{Tr}[\ddot{D}g] - \text{Tr}[\dot{D}g\dot{D}g] + 2\text{Tr}[\dot{D}g]^2) \rangle \\ &\quad - \langle \text{Tr}[g_{n0}\Gamma\gamma_5 g_{n0}^\dagger\gamma_5\Gamma^\dagger] \rangle \langle (\text{Tr}[\ddot{D}g] - \text{Tr}[\dot{D}g\dot{D}g] + 2\text{Tr}[\dot{D}g]^2) \rangle \} . \end{aligned} \quad (\text{A10})$$

APPENDIX B: FORMULAE FOR THE ISOVECTOR CHEMICAL POTENTIAL RESPONSE

Next, we consider responses to the isovector chemical potential, Eq.(16). In this case, the first derivative of Δ vanishes,

$$\dot{\Delta} = \frac{d}{d\hat{\mu}_V}(\det(D(\hat{\mu}_V))\det(D(-\hat{\mu}_V))|_{\hat{\mu}_V=0} = 0 \quad , \quad (\text{B1})$$

and the second derivative is obtained as

$$\frac{\ddot{\Delta}}{\Delta} = 2\text{Tr}[\ddot{D}g] - 2\text{Tr}[\dot{D}g\dot{D}g] \quad . \quad (\text{B2})$$

Similarly, derivatives of G are calculated as

$$\dot{G} = -2\text{ReTr}[(g\dot{D}g)_{n0}\Gamma\gamma_5 g_{n0}^\dagger\gamma_5\Gamma^\dagger] \quad , \quad (\text{B3})$$

and

$$\begin{aligned} \ddot{G} = 4\text{ReTr}[(g\dot{D}g\dot{D}g)_{n0}\Gamma\gamma_5 g_{n0}^\dagger\gamma_5\Gamma^\dagger] - 2\text{ReTr}[(g\ddot{D}g)_{n0}\Gamma\gamma_5 g_{n0}^\dagger\gamma_5\Gamma^\dagger] \\ + 2\text{Tr}[(g\dot{D}g)_{n0}\Gamma\gamma_5(g\dot{D}g)_{n0}^\dagger\gamma_5\Gamma^\dagger] \quad . \end{aligned} \quad (\text{B4})$$

Resulting expressions for the first and second responses to the isovector chemical potentials are

$$\frac{d}{d\hat{\mu}}\text{Re}\langle H(n)H(0)^\dagger \rangle = -2\text{ReTr}[(g\dot{D}g)_{n0}\Gamma\gamma_5 g_{n0}^\dagger\gamma_5\Gamma^\dagger] \quad , \quad (\text{B5})$$

and

$$\begin{aligned} \frac{d^2}{d\hat{\mu}^2}\text{Re}\langle H(n)H(0)^\dagger \rangle = 4\text{Re}\langle \text{Tr}[(g\dot{D}g\dot{D}g)_{n0}\Gamma\gamma_5 g_{n0}^\dagger\gamma_5\Gamma^\dagger] \rangle \\ - 2\text{Re}\langle \text{Tr}[(g\ddot{D}g)_{n0}\Gamma\gamma_5 g_{n0}^\dagger\gamma_5\Gamma^\dagger] \rangle \\ + 2\text{Re}\langle \text{Tr}[(g\dot{D}g)_{n0}\Gamma\gamma_5(g\dot{D}g)_{n0}^\dagger\gamma_5\Gamma^\dagger] \rangle \\ + 2\text{Re}\{ \langle \text{Tr}[g_{n0}\Gamma\gamma_5 g_{n0}^\dagger\gamma_5\Gamma^\dagger](\text{Tr}[\ddot{D}g] - \text{Tr}[\dot{D}g\dot{D}g]) \rangle \\ - \langle \text{Tr}[g_{n0}\Gamma\gamma_5 g_{n0}^\dagger\gamma_5\Gamma^\dagger] \rangle \langle (\text{Tr}[\ddot{D}g] - \text{Tr}[\dot{D}g\dot{D}g]) \rangle \} \quad . \end{aligned} \quad (\text{B6})$$

APPENDIX C: RESPONSES FOR STAGGERED FERMIONS

For staggered fermions, the determinant factor Δ is given by Eq.(20), and this leads to

$$\begin{aligned} \frac{\dot{\Delta}}{\Delta} &= \frac{1}{2}\text{Tr}[\dot{D}g] \quad , \\ \frac{\ddot{\Delta}}{\Delta} &= \frac{1}{2}\text{Tr}[\ddot{D}g] - \frac{1}{2}\text{Tr}[\dot{D}g\dot{D}g] + \frac{1}{4}\text{Tr}[\dot{D}g]^2 \quad . \end{aligned} \quad (\text{C1})$$

The final expressions for the second responses are

$$\begin{aligned}
\frac{d^2}{d\hat{\mu}^2} \text{Re}\langle H(n)H(0)^\dagger \rangle &= 4\text{Re}\langle \text{Tr}[(g\dot{D}g\dot{D}g)_{n0}\Gamma\gamma_5 g_{n0}^\dagger\gamma_5\Gamma^\dagger] \rangle \\
&\quad - 2\text{Re}\langle \text{Tr}[(g\ddot{D}g)_{n0}\Gamma\gamma_5 g_{n0}^\dagger\gamma_5\Gamma^\dagger] \rangle \\
&\quad - 2\text{Re}\langle \text{Tr}[(g\dot{D}g)_{n0}\Gamma\gamma_5 (g\dot{D}g)_{n0}^\dagger\gamma_5\Gamma^\dagger] \rangle \\
&\quad + 2\langle \text{ImTr}[(g\dot{D}g)_{n0}\Gamma\gamma_5 g_{n0}^\dagger\gamma_5\Gamma^\dagger] \text{ImTr}[\dot{D}g] \rangle \\
&\quad + \frac{1}{2}\text{Re}\{ \langle \text{Tr}[g_{n0}\Gamma\gamma_5 g_{n0}^\dagger\gamma_5\Gamma^\dagger] (\text{Tr}[\ddot{D}g] - \text{Tr}[\dot{D}g\dot{D}g] + \frac{1}{2}\text{Tr}[\dot{D}g]^2) \rangle \\
&\quad - \langle \text{Tr}[g_{n0}\Gamma\gamma_5 g_{n0}^\dagger\gamma_5\Gamma^\dagger] \rangle \langle (\text{Tr}[\ddot{D}g] - \text{Tr}[\dot{D}g\dot{D}g] + \frac{1}{2}\text{Tr}[\dot{D}g]^2) \rangle \} \quad (\text{C2})
\end{aligned}$$

for the isoscalar chemical potential, and

$$\begin{aligned}
\frac{d^2}{d\hat{\mu}^2} \text{Re}\langle H(n)H(0)^\dagger \rangle &= 4\text{Re}\langle \text{Tr}[(g\dot{D}g\dot{D}g)_{n0}\Gamma\gamma_5 g_{n0}^\dagger\gamma_5\Gamma^\dagger] \rangle \\
&\quad - 2\text{Re}\langle \text{Tr}[(g\ddot{D}g)_{n0}\Gamma\gamma_5 g_{n0}^\dagger\gamma_5\Gamma^\dagger] \rangle \\
&\quad + 2\text{Re}\langle \text{Tr}[(g\dot{D}g)_{n0}\Gamma\gamma_5 (g\dot{D}g)_{n0}^\dagger\gamma_5\Gamma^\dagger] \rangle \\
&\quad + \frac{1}{2}\text{Re}\{ \langle \text{Tr}[g_{n0}\Gamma\gamma_5 g_{n0}^\dagger\gamma_5\Gamma^\dagger] (\text{Tr}[\ddot{D}g] - \text{Tr}[\dot{D}g\dot{D}g]) \rangle \\
&\quad - \langle \text{Tr}[g_{n0}\Gamma\gamma_5 g_{n0}^\dagger\gamma_5\Gamma^\dagger] \rangle \langle (\text{Tr}[\ddot{D}g] - \text{Tr}[\dot{D}g\dot{D}g]) \rangle \} \quad (\text{C3})
\end{aligned}$$

for the isovector chemical potential.

REFERENCES

- [1] M. A. Stephanov, Phys. Rev. Lett. **76**, 4472 (1996).
- [2] T. Hatsuda and S. H. Lee, Phys. Rev. **C46**, R34 (1992).
- [3] A. Hayashigaki, Phys. Lett. **B487**, 96 (2000).
- [4] CERES collaboration: G. Agakishv *et al.*, Nucl. Phys. **A638**, 159 (1998).
- [5] NA50 collaboration: M. C. Abreu *et al.*, Phys. Lett. **B477**, 28 (2000); See also H. Satz, Nucl. Phys. **B(Proc.Suppl.) 94**, 204 (2001).
- [6] R. Rapp and Ch. Gale, Phys. Rev. **C60**, 024903 (1999); J. Stachel, Nucl. Phys. **A654**, 119c (1999); R. Rapp and J. Wambach, nucl-th/0001014.
- [7] I. M. Barbour, S. E. Morrison, E. G. Klepfish, J. B. Kogut, and M. Lombardo, Nucl. Phys. **B(Proc.Suppl.) 60A**, 220 (1998).
- [8] F. Karsch, Nucl. Phys. **B(Proc.Suppl.) 83**, 14 (2000); O. Kaczmarek, J. Engels, F. Karsch, and E. Laermann, Nucl. Phys. **B(Proc.Suppl.) 83**, 369 (2000); G. Aarts, F. Karsch, O. Kaczmarek and I.-O. Stamatescu, “First order correction to quenched QCD at non-zero chemical potential”, in preparation.
- [9] S. Gottlieb *et al.*, Phys. Rev. **D55**, 6852 (1997).
- [10] QCDTARO-collaboration: Ph. de Forcrand *et al.*, Nucl. Phys. **B(Proc.Suppl.) 63A-C**, 460 (1998).
- [11] QCDTARO-collaboration: Ph. de Forcrand *et al.*, Nucl. Phys. **B(Proc.Suppl.) 73**, 477 (1999).
- [12] S. Gottlieb *et al.*, Phys. Rev. **D38**, 2888 (1988).
- [13] D. T. Son and M. A. Stephanov, Phys. Rev. Lett. **86**, 592 (2001).
- [14] M. Fukugita *et al.*, Phys. Rev. **D42**, 2936 (1990).
- [15] S. Gottlieb *et al.*, Phys. Rev. **D35**, 3972 (1987).
- [16] S. J. Dong and K. F. Liu Phys. Lett. **B328**, 130 (1994).
- [17] S. Gottlieb *et al.*, Phys. Rev. **D47**, 3619 (1993).
- [18] CP-PACS Collaboration : A. Ali *et al.*, hep-lat/0103028.
- [19] O. Miyamura and S. Choe, hep-ph/0105198.

TABLES

TABLE I. Parameters of the simulations. $\#conf.$ stands for the number of configurations analyzed.

ma	β	$\#conf.$	T
0.0125	5.26	600	$0.99T_C$
	5.34	300	$1.10T_C$
0.0170	5.26	600	$0.98T_C$
	5.34	300	$1.09T_C$
0.0250	5.20	600	$0.89T_C$
	5.26	600	$0.96T_C$
	5.32	300	$1.05T_C$
	5.34	300	$1.07T_C$

TABLE II. Responses of the pseudoscalar meson to the isoscalar chemical potential $\hat{\mu}_S$.

ma	β	\hat{M}	$\frac{1}{A} \frac{d^2 A}{d\hat{\mu}^2}$	$\frac{d^2 \hat{M}}{d\hat{\mu}^2}$	$\frac{1}{\hat{\gamma}} \frac{d^2 \hat{\gamma}}{d\hat{\mu}^2}$
0.0125	5.26	0.2956(2)	-1.4(20)	0.17(35)	-0.8(23)
	5.34	0.7513(11)	-4.23(49)	5.39(10)	2.95(51)
0.0170	5.26	0.3506(2)	-1.5(14)	0.30(26)	-0.6(16)
	5.34	0.7421(35)	-3.68(75)	5.82(16)	4.16(78)
0.0250	5.20	0.4061(2)	-0.4(14)	0.16(26)	0.0(16)
	5.26	0.4218(2)	-0.8(11)	0.29(20)	-0.1(12)
	5.32	0.6926(11)	-4.65(91)	5.17(20)	2.82(96)
	5.34	0.7534(7)	-3.17(41)	4.43(8)	2.71(42)

TABLE III. Responses of the pseudoscalar meson to the isovector chemical potential $\hat{\mu}_V$.

ma	β	$\frac{1}{A} \frac{dA}{d\hat{\mu}}$	$\frac{d\hat{M}}{d\hat{\mu}}$	$\frac{1}{A} \frac{d^2 A}{d\hat{\mu}^2}$	$\frac{d^2 \hat{M}}{d\hat{\mu}^2}$	$\frac{1}{\hat{\gamma}} \frac{d^2 \hat{\gamma}}{d\hat{\mu}^2}$
0.0125	5.26	0.0029(57)	-0.0001(12)	47.46(71)	-12.93(43)	3.7(16)
	5.34	0.0047(93)	0.0006(21)	2.32(64)	-1.32(32)	0.56(77)
0.0170	5.26	-0.0081(48)	-0.0005(10)	33.52(61)	-10.49(33)	3.6(11)
	5.34	0.0000(82)	-0.0012(19)	2.74(64)	-1.48(32)	0.75(78)
0.0250	5.20	0.0062(39)	0.0016(8)	25.24(46)	-9.10(23)	2.84(74)
	5.26	-0.0080(37)	0.0007(8)	23.22(46)	-8.64(23)	2.72(71)
	5.32	-0.0054(64)	-0.0020(14)	4.04(75)	-2.14(38)	0.95(93)
	5.34	0.000(6)	0.000(1)	2.99(53)	-1.51(26)	0.99(60)

FIGURES

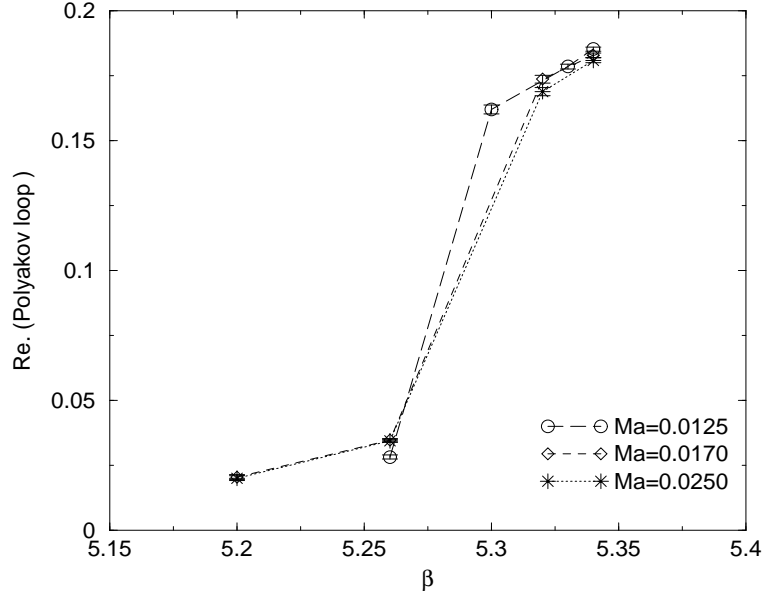


FIG. 1. Average value of the Polyakov loop as a function of β .

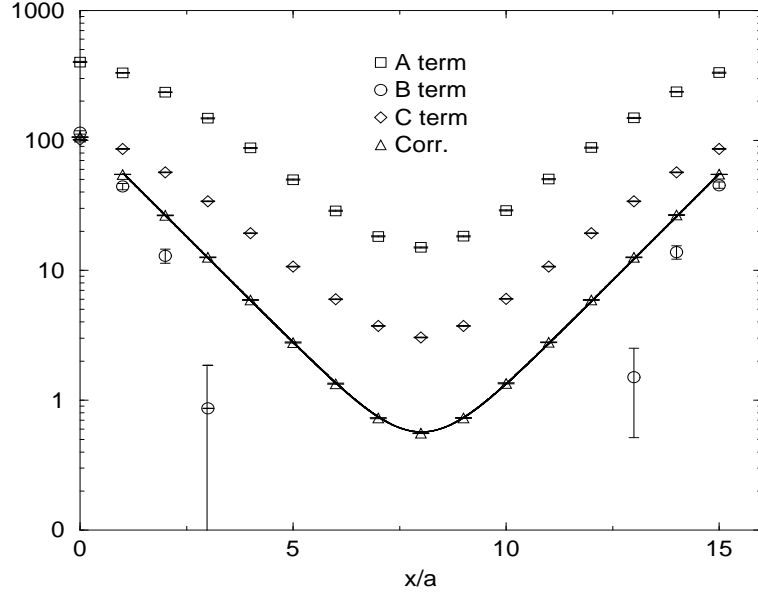


FIG. 2. Pseudoscalar correlator and some contributions to its response to $\hat{\mu}_{S,V}$ (see Eq.(21)) at $\beta = 5.34$ and $ma = 0.025$. The correlator is fitted by the single pole formula Eq.(2).

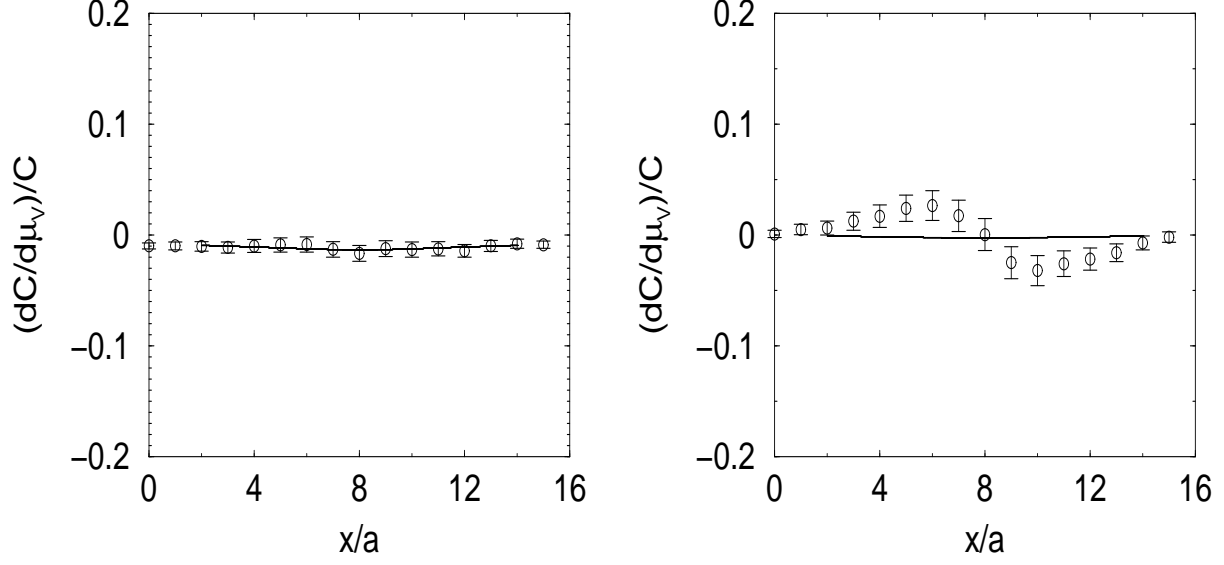


FIG. 3. The first response of the pseudoscalar meson correlator at $\beta = 5.26$ ($T < T_c$, left) and $\beta = 5.34$ ($T > T_c$, right). The quark mass is $ma = 0.025$.

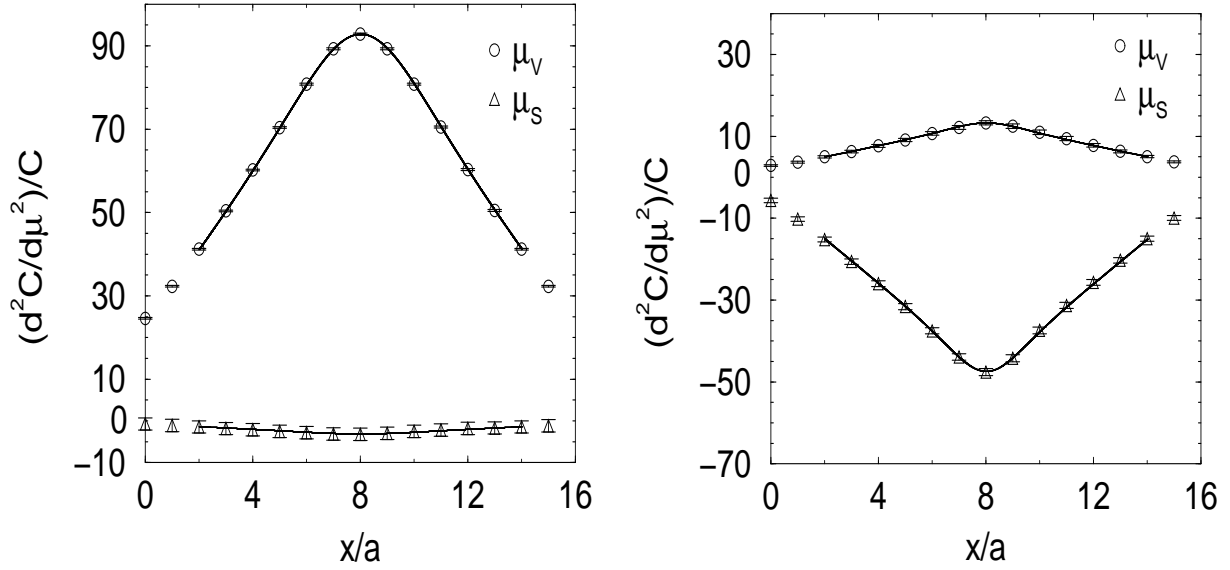


FIG. 4. The second response of the pseudoscalar meson correlator at $\beta = 5.26$ and $ma = 0.025$ ($T < T_c$, left), and at $\beta = 5.34$ and $ma = 0.0125$ ($T > T_c$, right). The curves are fits to Eq.(4).

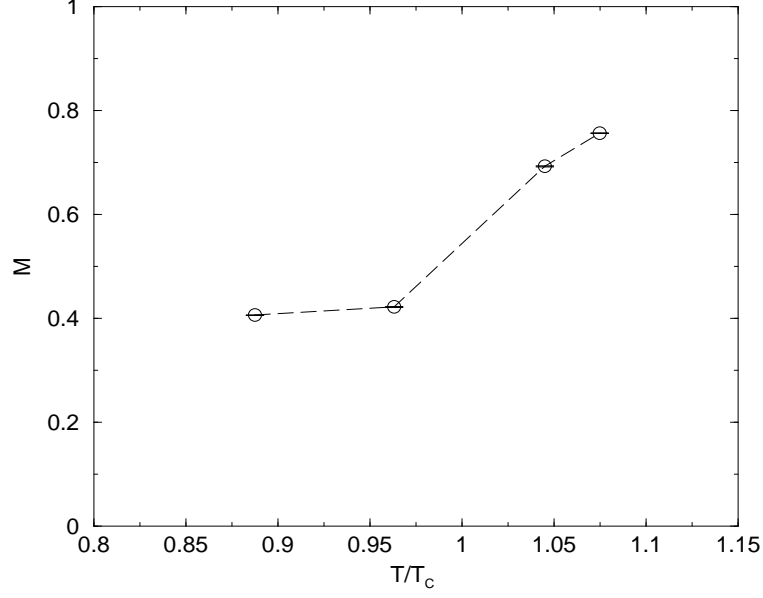


FIG. 5. Screening mass of the pseudoscalar meson at $ma = 0.025$, in a^{-1} units. β_C is taken from Ref.[15]. Values for T/T_C are estimated by using the two-loop β -function.

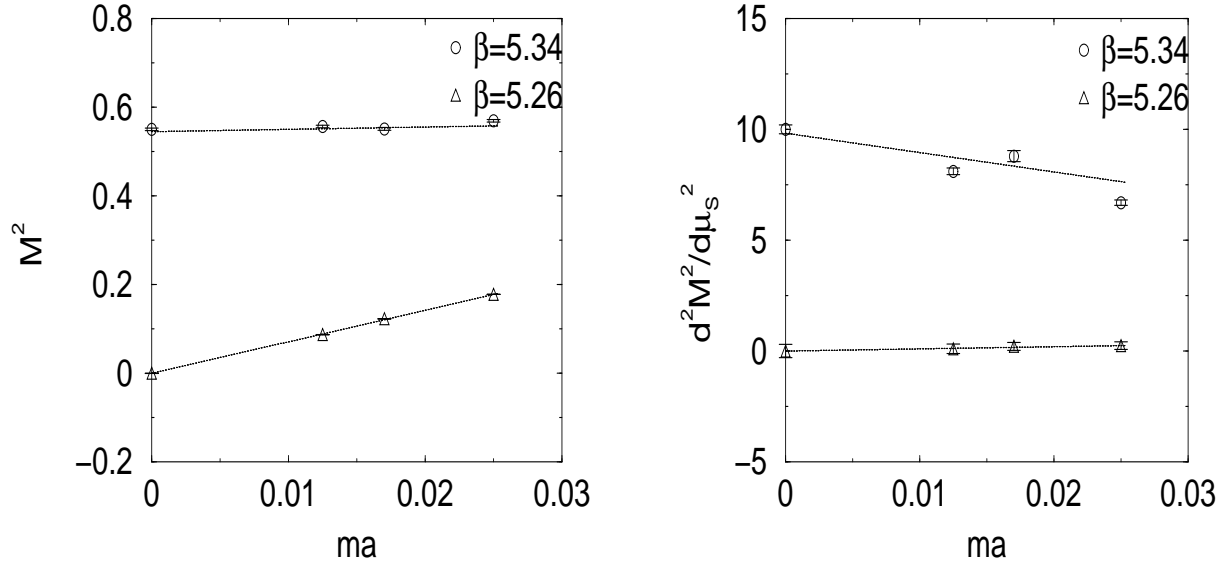


FIG. 6. \hat{M}^2 (left) and $d^2 \hat{M}^2 / d \hat{\mu}_S^2$ (right) for the pseudoscalar meson versus ma . β is 5.26 (triangles) and 5.34 (circles). Extrapolation to $ma = 0$ is also shown.

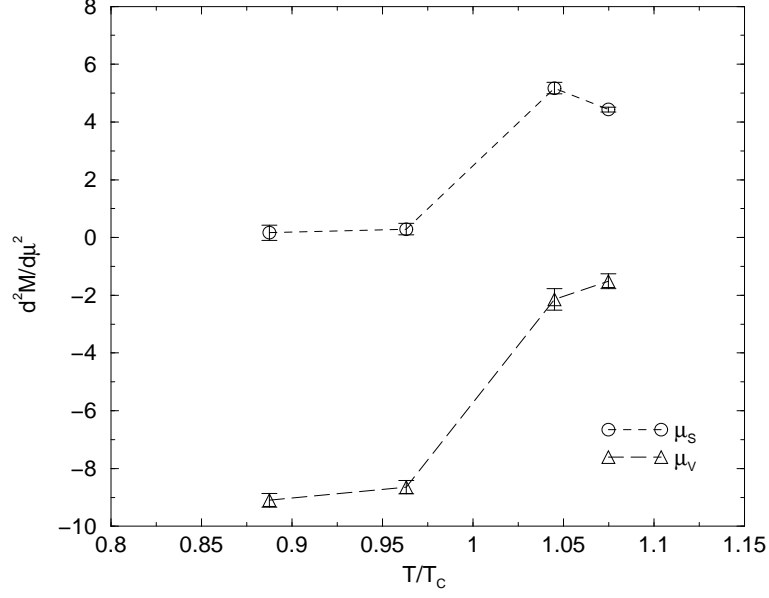


FIG. 7. Second response $d^2 \hat{M} / d \hat{\mu}_S^2$, $d^2 \hat{M} / d \hat{\mu}_V^2$ of the pseudoscalar meson at $ma = 0.025$. T/T_c is estimated as in Fig.5.

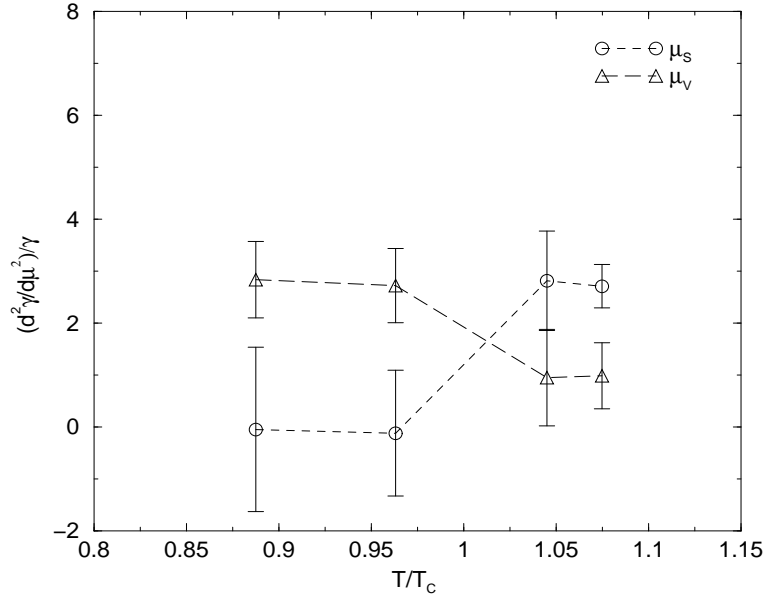


FIG. 8. Second response of the coupling, $\hat{\gamma}^{-1} d^2 \hat{\gamma} / d \hat{\mu}_S^2$, $\hat{\gamma}^{-1} d^2 \hat{\gamma} / d \hat{\mu}_V^2$, for the pseudoscalar meson at $ma = 0.025$. T/T_c is estimated as in as Fig.5.

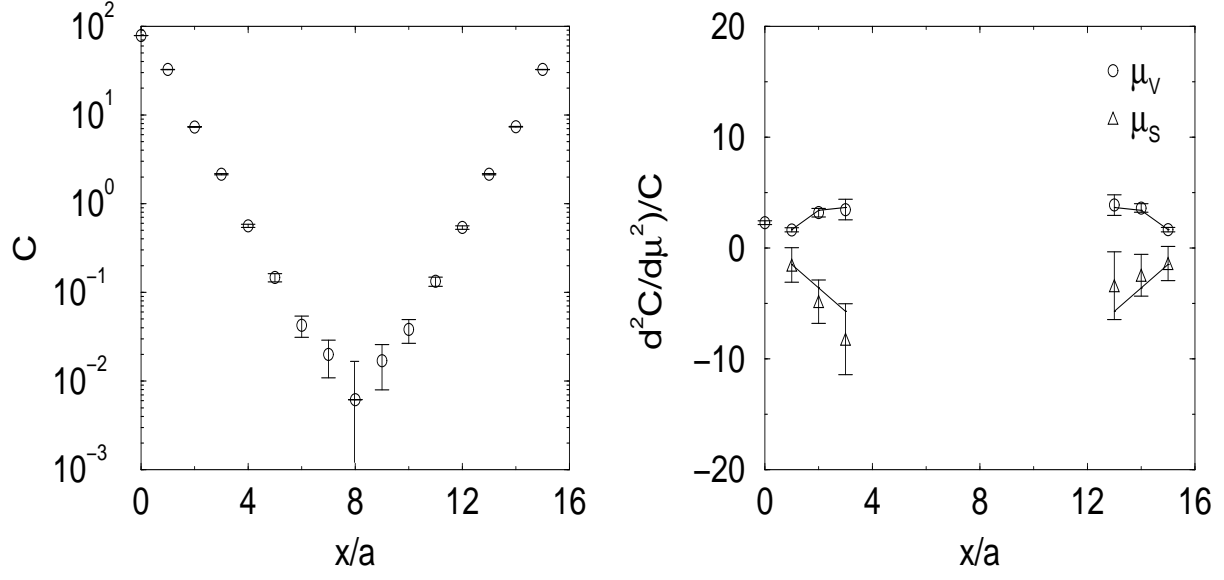


FIG. 9. Vector meson correlator at $\beta = 5.26$ and $ma = 0.025$ (left), and its second response (right).